Journal of the Physical Society of Japan
Vol. 59, No. 3, March, 1990, pp. 1047–1058

Soliton Lattice Modulation of Incommensurate Spin Density Wave in Two Dimensional Hubbard Model —A Mean Field Study—

Masaru KATO, Kazushige MACHIDA,† Hiizu NAKANISHI††,* and Mitsutaka FUJITA†††

Department of Mathematical Sciences, College of Engineering, University of Osaka Prefecture, Mozu, Sakai-shi 591
†Department of Physics, Kyoto University, Kyoto 606
††Institute of Theoretical Physics, University of California, Santa Barbara, California 93106, U.S.A.
†††Institute of Materials Science, University of Tsukuba, Tsukuba 305

(Received August 24, 1989)

Spatially modulated magnetic phases are investigated within the mean field theory for an itinerant electron model, i.e. the Hubbard model on a two-dimensional square lattice. By numerically diagonalizing the Hamiltonian for finite-size systems under a periodic boundary condition, we examine relative stability and physical properties of several possible magnetic states. When the electron fillings are nearly half-full, the diagonally or vertically modulated spin density wave (SDW) state is stabilized over the uniform antiferromagnetic state and a crossover from the vertical to the diagonal states appears. The diagonal or vertical stripe state is characterized by the presence of the midgap band due to the soliton lattice formation inside the main SDW gap, being an insulator. The wave length λ_{SDW} is linearly proportional to the excess carrier concentration. Excess carriers are accommodated in the form of the soliton lattice, forming a charge density wave whose wave length is $\lambda_{SDW}/2$.

§1. Introduction

Much attention has been focused on the behaviors of excess carriers (holes or electrons) introduced in CuO_2 planes of high T_c oxide superconductors. It is established experimentally that the mother compounds for high T_c oxides such as La_2CuO_4, Nd_2CuO_4 or $YBa_2Cu_3O_6$ commonly exhibit antiferromagnetic long range order. In the case of $La_{2-x}A_xCuO_4$ (A: Sr or Ba) which is the most extensively studied system an incommensurate modulated magnetic quasi-static order is observed as doping proceeds even in the superconducting samples ($x \sim 0.15$) by neutron experiments.[1)]

Here we take up the Hubbard model in two dimensions (2D) where electrons are nearly half-full as a model for describing a d-p hybridized band on a CuO_2 plane. Although this system is often discussed from the strong correlation limit where several interesting physics are emerging, the actual oxide systems may be neither strong correlation limit nor weak coupling limit, but intermediate at best. It should be recognized that even in the weak coupling region the Hubbard model is poorly studied so far, especially when the electron filling is away from the exactly half-full, which corresponds to the actual situation of doped cases where the high T_c superconductivity occurs. Long time ago Penn[2)] studied the relative stability of various magnetic phases all of which are uniform in space: antiferromagnetic (AF), ferromagnetic (FM), or ferrimagnetic states, etc within the mean field approximation in three dimensions.

It is now evident from the progress of so-called soliton physics in magnetic systems[3,4)] that spatially modulated phases are more ad-

* Present address: Department of Physics, Faculty of Science and Technology, Keio University, Hiyoshi, Kohoku-ku, Yokohama 223.

vantageous energetically than the uniform phases in order to neatly accommodate excess electrons (more than half-filling as in electron-doped system (Nd, Ce)$_2$CuO$_4$) or holes (less than half-filling as in hole-doped system (La, Sr)$_2$CuO$_4$). In contrast, the ground state in the 2D Hubbard model with the exactly half-filling is believed to be antiferromagnetic both in weak and strong correlation cases. In fact, several authors[5] show that a few holes introduced destroy locally the AF state as a background, supporting an idea of the "spin-bag" due to Schrieffer *et al.*[6]

Similar studies on the 2D Hubbard model with a finite number of holes as ours are emerging concurrently by Poilblanc and Rice,[7] Schulz,[8] and Zaanen and Gunnarsson.[9] They, including ours, are complementary to each other. We also mention a recent result due to Monte Carlo simulation on the 2D Hubbard model that Imada and Hatsugai[10] found an incommensurately modulated magnetic correlation in non half-filling cases, which differs from the earlier results by Hirsch and Tang[11,12] and White *et al.*[13]

Here we address several questions concerning the 2D Hubbard model on a square lattice with electron fillings off the half-full:

(1) How are excess carriers (electrons or holds) accommodated in a system?

(2) Which state is most stable among various possible magnetic phases, in particular, the single Q state or double Q state? The former breaks the square symmetry while the latter preserves it.

(3) What are properties of a soliton lattice state which we are going to find; the energy gap structure, magnetic pattern of spatial modulation etc.?

In order to answer these questions we try to find the most stable magnetic phase by solving a self-consistent equation numerically for finite size systems within the mean field approximation. It turns out the phase diagram (interaction constant vs electron filling) obtained earlier, which was taken into account only spatially uniform phases, is drastically changed.

§2. Mean Field Theory

We start with the Hubbard model on a two-dimensional square lattice:

$$H=-t\sum_{\langle ij\rangle\sigma} c_{i\sigma}^{\dagger}c_{j\sigma}+U\sum_i n_{i\uparrow}n_{i\downarrow}, \tag{1}$$

where $\langle ij\rangle$ denotes the sum over nearest neighbor sites. At the half filling ($n=1$) where n is the electron number per site the uniform antiferromagnetic order is most stable phase at least within the mean field approximation, where the up-spin electrons are uniformly distributed on one of the bipartital sublattice A (or B) and thus the ground state is doubly degenerate. Here we consider the situation in which the electron filling n is slightly less ($n\lesssim 1$) or more ($n\gtrsim 1$) than half-full. From the symmetry consideration (charge conjugation symmetry: $n\lessgtr 1$ symmetry) we concentrate on the $n\lesssim 1$ case. A mean field Hamiltonian of (1) can be written as

$$H_{MF}=-t\sum_{\langle ij\rangle\sigma} c_{i\sigma}^{\dagger}c_{j\sigma}+\sum_i\Big\{(\langle\rho_i\rangle-\langle M_i\rangle)n_{i\uparrow} +(\langle\rho_i\rangle+\langle M_i\rangle)n_{i\downarrow}-\frac{1}{U}(\langle\rho_i\rangle^2-\langle M_i\rangle^2)\Big\}, \tag{2}$$

where we have defined the charge density $\langle\rho_i\rangle$ and spin density $\langle M_i\rangle$ at a lattice site i by

$$\langle\rho_i\rangle=\frac{U}{2}(\langle n_{i\uparrow}\rangle+\langle n_{i\downarrow}\rangle), \tag{3}$$

$$\langle M_i\rangle=\frac{U}{2}(\langle n_{i\uparrow}\rangle-\langle n_{i\downarrow}\rangle). \tag{4}$$

The spin direction is assumed to be unique (say, z-direction). We disregard the possibility of a non-collinear spin arrangement. This choice is plausible because the sinusoidal spin density wave (SDW) is more stable than the helically modulated phase within the framework of the itinerant model[4] although we cannot completely exclude the possibility of some non-collinear phase. We allow the site-dependence of the charge $\langle\rho_i\rangle$ and spin $\langle M_i\rangle$ densities which are determined self-consistently by eqs. (3) and (4). Note that the simple AF is to assume the uniform spin density on each sublattice A and B of the bipartital square lattice.

In order to find stable spin and charge configurations which satisfy the self-consistency requirement, we have numerically diagonalized the mean field Hamiltonian for finite-size systems under the periodic boundary

condition in direct space; Starting with an appropriate initial configuration as an input, we employ the simple iteration method to seek a self-consistent solution. Namely we first diagonalize the Hamiltonian matrix ($N^2 \times N^2$) where we are considering a square-shaped system with $N \times N$ sites to find the eigenvalues and eigenfunctions (N is even). Then evaluate various averages $\langle \rho_i \rangle$ and $\langle M_i \rangle$ by filling electrons from the lower energy eigenvalues in order to check the self-consistency. If failed, starting again with the renewed initial configuration, we repeat the same process until a certain convergence condition is cleared. We did not impose the condition a priori during this process that the numbers of up-spin electrons and down-spin electrons be same. However, our self-consistent solutions always result in yielding the same up and down electron numbers. As a general tendency, the convergence is easily attained when U becomes large and the filling is near the half-filling if we carefully choose an appropriate combination of the electron filling (or hole number) and the system size, such as the hole number $1-n=2/N$ for a $N \times N$ system, otherwise it is almost impossible to reach a local minimum configuration or a self-consistent solution by the present simple iteration method.

The maximum size in our calculations was 20×20 sites. We varies the normalized interaction constant $u(\equiv U/t)$ and hole concentration n near the half-filling. We have checked the size-dependence of our results by seeing that the total energies per site of the systems for a spin configuration are independent of the system size and also that under a fixed hole concentration the stable spin configuration is independent of the system size. In Figs. 1(a) $\sim$1(d) we illustrate an example where $n=0.8$ and $u=8.0$, the same spin patterns (a)$\sim$(c) and the same level distributions (d) are obtained as a stable solution, for different sizes (5×5, 10×10 and 20×20). In this example the total energies per electron normalized by t are -2.453 for 5×5 system, -2.452 for 10×10 system and -2.442 for 20×20 system where the total energy E_{total} is defined in Table I.

§3. Possible Magnetic Phases

In this section we introduce several possible magnetic phases among which we select out the most stable state in the U vs n plane.

The uniform antiferromagnetic state (AF) is stable in the exactly half filling. The earlier mean field calculation[12] indicates that AF is stable over the substantial region in the n vs U plane as will be seen in Fig. 5 where we refer to the phase diagram Fig. 3. in ref. 12). However, it is evident that AF could be unstable against some incommensurate spin density wave states.

(1) Diagonal stripe state

Since the dispersion curve of the non-interacting system is give by

$$\varepsilon(k_x, k_y) = -2t(\cos k_x + \cos k_y), \tag{5}$$

the Fermi surface nesting situation near the half-filling is expected to be good for a wave vector $Q=(\pi-\delta, \pi-\delta)$ whose direction is diagonal to the underlying square lattice. The wave number deviation δ from the commensurate value (π, π) is proportional to the hole concentration; $\delta=2\pi/N$ and is incommensurate with the host lattice in general (the lattice constant is unity). Namely under a condition of the fixed electron number at $T=0$ the system always favors an incommensurate $\boldsymbol{Q}$ vector.

(2) Vertical stripe state

The paramagnetic susceptibility $\chi(\boldsymbol{q})$ defined by

$$\chi(\boldsymbol{q}) = -\sum_{\boldsymbol{k}} \frac{f(\varepsilon(\boldsymbol{k})) - f(\varepsilon(\boldsymbol{k}+\boldsymbol{q}))}{\varepsilon(\boldsymbol{k}) - \varepsilon(\boldsymbol{k}+\boldsymbol{q})}, \tag{6}$$

with $f(x)$ being the Fermi distribution function is maximum when $\boldsymbol{q}=\boldsymbol{Q}=(\pi, \pi \pm \delta)$ because toward the half-filling the density of states becomes large due to the presence of the van Hove singularity at the half-filling (see for example ref. 8)). The modulation of the spin arrangement corresponding to this wave vector propagates along y or x axis of the square lattice.

(3) Cross stripe state

Since the Fermi surface in the paramagnetic state is square-symmetric, a symmetry adapted spin arrangement is also expected to appear, in particular, far away from the half-filling in which situation the nesting for the single $\boldsymbol{Q}$ vector becomes worse while the double $\boldsymbol{Q}$ vectors become more favorable. Two nesting vectors;

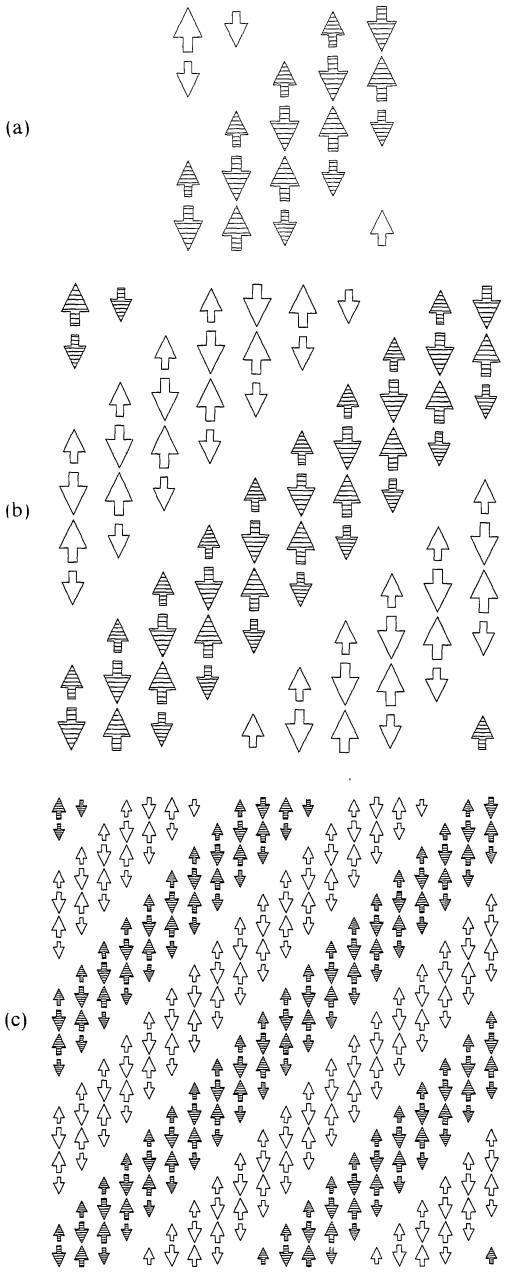

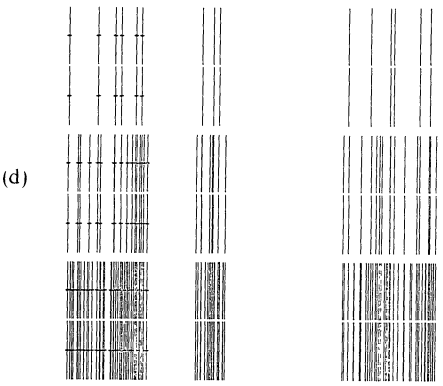

Fig. 1. Examples of the numerical results which illustrate that the same stable configuration (diagonal stripe state) with different system sizes (5×5, 10×10 and 20×20 sites) is obtained. $n=0.8$ and $u=8.0$. Magnetization (or spin) profiles for 5×5 site system (a), 10×10 site system (b) and 20×20 site system (c). The length of arrows is proportional to the magnitude of the spin at a site. The different symbols (shaded and unshaded arrows) indicate two kinds of the domains (A and B). The patterns of the 5×5 system and the 10×10 system are embedded in that of the 20×20 system. (d) The eigenvalue distributions of the up and down spin electrons (upper and lower portions) for the above systems (5×5, 10×10, and 20×20 systems from top to bottom); A bar corresponds to an eigenvalue. From left to right the energy of the eigenvalues is increased. The small dots on a bar denote that eigenstate is occupied by electrons.

$(\pi-\delta, \pi-\delta)$ and $(-\pi+\delta, \pi-\delta)$ which are perpendicular to each other are superposed to form a cross stripe spin modulation on the square lattice. Indeed Fenton[14] and Buker[15] independently discuss the stability condition for multi-Q state vs single Q state in detail in three dimensional systems.[16]

§4. Relative Stability of Selected Magnetic States

We have performed numerical computations to solve the self-consistent equation (2) and to know the nature of the modulated states. We also examined the relative stability in selected points on the n vs u plane by comparing the ground state energies for the three

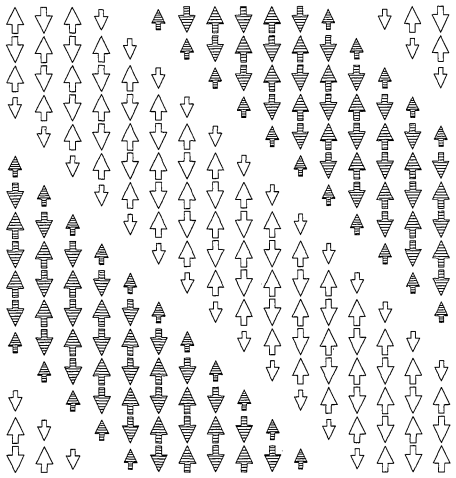

(a)

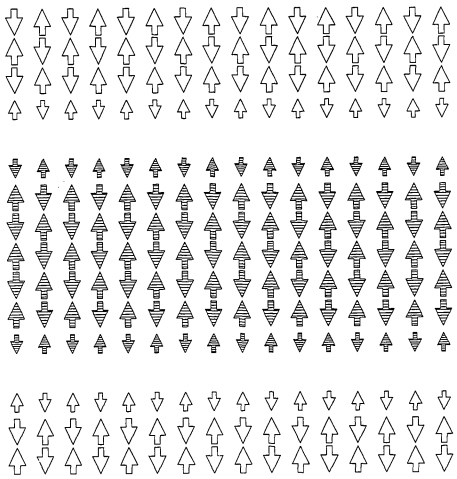

(b)

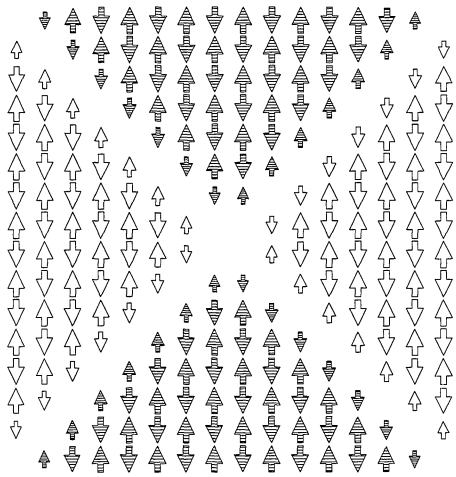

(c)

Fig. 2. Three stable spin configurations for $n=0.875$, $u=8.0$ and system size; 16×16 sites: (a) The diagonal stripe state; The spin modulation propagates diagonally to the underlying square lattice. The domain walls (or lines), namely soliton lines are perpendicular to the modulation and periodically placed. The domains A and B are alternate. Inside each domain almost simple antiferromagnetic pattern is realized. (b) The vertical stripe state; The spin modulation propagates vertically to the underlying square lattice. The domain walls or soliton lines run horizontally. Almost no horizontal modulation is seen in this scale. (c) The cross stripe state; The spatial pattern is described by two modulation vectors which are orthogonal to each other. The soliton also are orthogonal to each other.

possible magnetic phases mentioned above.

In Fig. 2 we display three examples of the results for a fixed system size (16×16) calculated under the same conditions: The interaction constant $u=8.0$, electron filling $n=0.875$. These three states clear a certain convergence condition to ensure the local energy minimum solution of the self-consistent equation (2) and are also confirmed to be more stable than the uniform AF state. In this particular case the diagonal stripe state (Fig. 2(a)) has the lowest energy among the three configurations. The cross stripe state (Fig. 2(c)) which preserves the square symmetry is intermediate and the vertical (or equivalently horizontal) stripe state (Fig. 2(b)) is highest.

The spatial modulation of these states is characterized by a domain wall (line) which connects the doubly degenerate AF ground state, namely between $\uparrow\downarrow\uparrow\downarrow$ sequence and $\downarrow\uparrow\downarrow\uparrow$ sequence. We used in Fig. 2 different symbols (shaded and unshaded arrows) to distinguish these two domains. The size of these arrows is proportional to the magnitude of the magnetization $\langle M_i\rangle$ at a site i. It is seen that (1) Near the domain wall or antiphase boundary the magnetization rapidly changes and vanishes. (2) Far away from the domain wall the magnetic structure is almost antiferromagnetic. (3) Along the direction perpendicular to the propagation vector $\boldsymbol{Q}$ almost no spatial variation of the magnetization occurs.

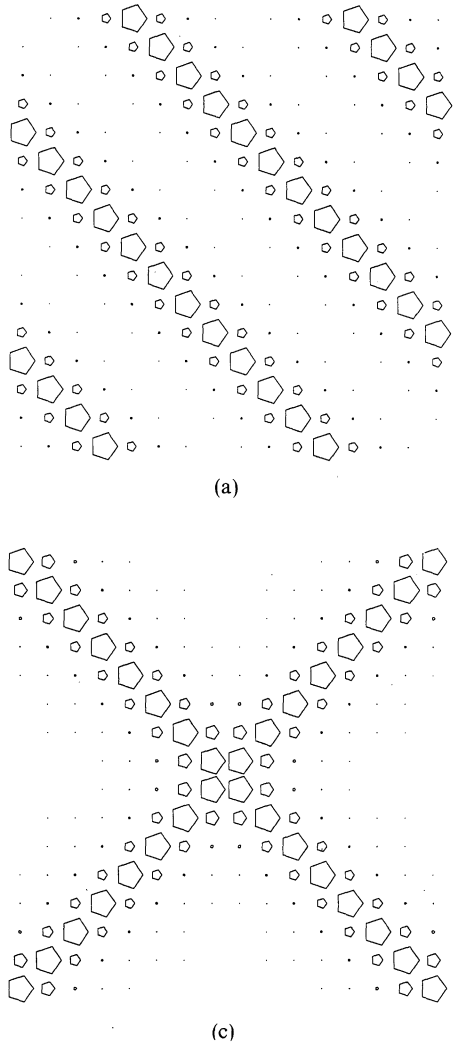

Fig. 3. Three charge density patterns $\delta\rho_i$ associated with the three spin configurations in Fig. 2 ($n=0.875$, $u=8.0$ and the system size 16×16 are same). (a) The diagonal stripe state; The excess carriers or holes are accumulated along the soliton line. (b) The vertical stripe state; Holes line up horizontally. (c) The cross stripe state; Holes form a cross pattern.

These three patterns correspond to the magnetic states; diagonal, vertical and cross stripe states respectively introduced in the previous section.

The charge distributions $\delta\rho_i=|\langle\rho_i\rangle-\rho_{\max}|/t$ with $\rho_{\max}=\max\langle\rho_i\rangle$ corresponding to each magnetic states in Fig. 2 are shown in Fig. 3 where the parameters used are same. It is clearly seen that the charge distribution is regularly arranged in direct space to form a charge density wave (CDW) whose wave number is exactly twice the SDW wave number Q. The excess charges introduced into the system are accommodated in the domain wall and line up next to each other, forming a charge rod. In the cross stripe state (Figs. 2(c) and 3(c)) these charged rods are intersected to lose the repulsive energy because of the over-accumulation of excess charges at a crossing site, making this state less advantageous over the other single Q stripe states in this sense. However, in the electron fillings far away from the half-full the cross stripe state may be stabilized.

As will be discussed in detail for the single Q stripe state in the next section the wave number Q is linearly proportional to the deviation from the half-filling, namely $Q\propto|1-n|$; the excess charge number. As U increases the width of the domain wall becomes sharper and the envelope function of the spatial variation tends to be step function-like.

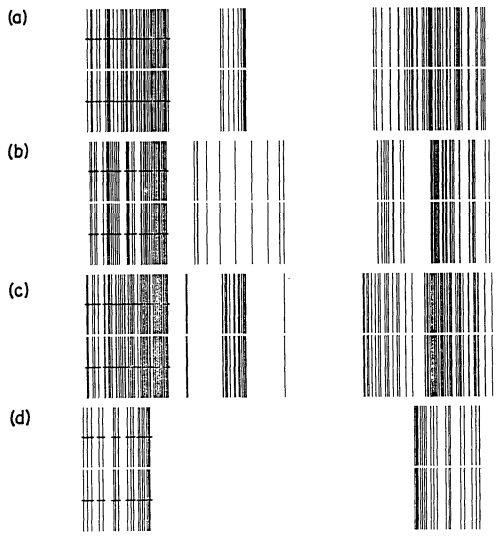

Fig. 4. The eigenvalue distributions for various states corresponding to Figs. 2 and 3. ($u=8.0$, $n=0.875$ and 16×16 system). (a) The diagonal stripe state. (b) The vertical stripe state. (c) The cross stripe state. (d) The uniform antiferromagnetic state (in the case of $n=1.0$).

In Fig. 4 we plot the eigenvalue distribution for each magnetic states with the same set of the parameters as in Figs. 2 and 3. They are mainly grouped into three bands; the lowest band is occupied and separated by a gap from the remaining unoccupied bands, forming the valence band. The unoccupied top band forms the conduction band which is separated by the main large energy gap of the SDW from the valence band. In the middle of the level distribution a midgap band appears for all stripe states in common although their band widths differ from each other. The midgap band is empty for less-than-half case to accommodate holes while occupied for more-than-half case. It should be noted that these three states are commonly an insulator because the occupied valence band is separated by a SDW gap. There is no Fermi surface remained. This is contrasted with the uniform AF in non-half filling case where the Fermi surface always appears, loosing the AF condensation energy: This is one of the main reason why the non-uniform states are stabilized when the filling is off the half-filling.

We have observed a crossover of the most stable state from the diagonal stripe state to the vertical stripe one as U decreases under a fixed electron filling. This phenomenon is also pointed out by Schulz.[8] The crossover occurs at around $u_{cr}\sim5$ depending on the filling as seen from Table I. As n increases toward $n=1$, u_{cr} tends to decrease. This conclusion does not depend on the system sizes which we have checked ($12\times12\sim16\times16$). As far as we have searched ($3\leqq u\leqq8$) there is no stable region of the cross stripe state in the diagram u vs n, which is indeed a local minimum state yet.

We also notice important changes from the previously known phase diagram referred to in Fig. 5 that (1) there is no stable region of the uniform AF in n vs U, except, of course, for the exactly half-filling $n=1$ where the simple AF is most stable. (2) We also found a region previously known as the paramagnetic region in the phase diagram where the vertical stripe is more stable than the paramagnetic state. The phase diagram should be altered so as to extend the ordered region, that is, the "old" phase boundary between the uniform AF and the paramagnetic state depicted in Fig. 5 should be moved downwordly. This is expected because we have found more stable states than the uniform AF. In Fig. 5 we plot the points we have checked in which either

Table I. Comparison of the total energies of various phases; diagonal, vertical, cross stripe states and the uniform antiferromagnetic state (AF) for the selected points in u vs n. The system sizes are 10×10 and 16×16 sites where the total energy E_{total}/t is defined by $E_{total}=\langle H_{MF}\rangle-\frac{1}{4}UN(1-n)^2$.

Size	U/t	n	Diagonal	Vertical	Cross	AF
10×10	4	0.8	−160.47	−161.74	—	−159.30
	6	0.8	−175.33	−174.43	—	−168.17
	8	0.8	−196.16	−193.97	—	−185.25
16×16	4	0.875	−429.10	−429.20	−428.97	−422.68
	8	0.875	−545.99	−542.29	−544.25	−526.91

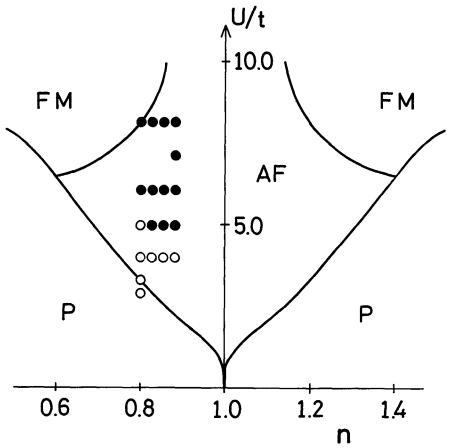

Fig. 5. The phase diagram (U/t vs n) calculated previously (Fig. 3 in ref. 12), where FM, AF and P denote the ferromagnetic, antiferromagnetic and paramagnetic states respectively. The points indicate the calculated points; A filled (empty) circle denotes that the diagonal (vertical) stripe state is most stable at that point. We notice that an empty circle at $n=0.8$ and $u=3.0$ indicates that the vertical stripe state is most stable at this point in the phase diagram; The "true" phase boundary between the paramagnetic and ordered states should lie outside the "old" phase boundary depicted here.

diagonal stripe (filled circle) or vertical stripe (empty circle) states are confirmed to be more stable than the uniform AF as the ground state.

§5. Nature of the Stripe State

Having seen that the single Q stripe state, either diagonal or vertical one is most stable near the half-filling, let us consider the physical nature of the state in detail. We take up mainly the diagonal stripe state as an example and compare it with the vertical stripe state.

5.1 Band structure

We show in Fig. 6 the overall level or band structure of the stripe states as a function of U under a fixed filling ($n=0.875$) where the energy scale is normalized by the total band width W. It is seen that the band is grossly devided into three parts where the lowest band is occupied and the other are empty. As U decreases the position of the midgap band tends to approach the center of the total band or the main gap. We note that the original

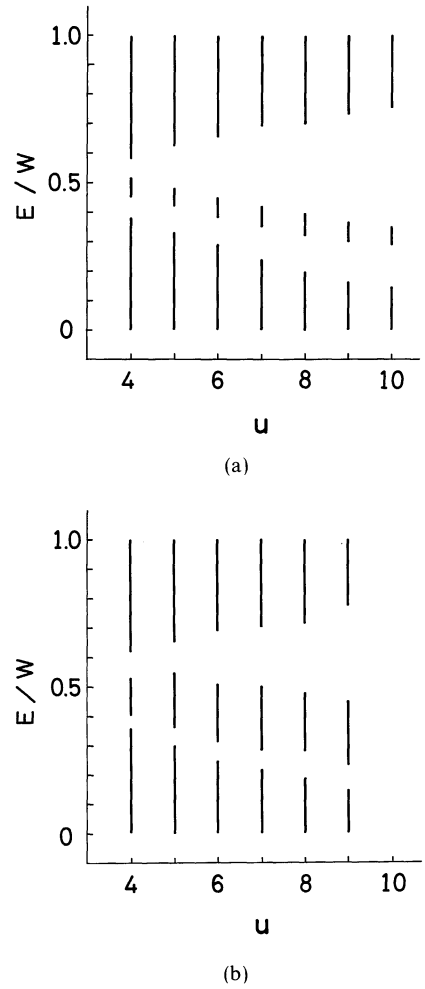

Fig. 6. The overall band structures or the eigenvalue distributions normalized by the band width W as a function of u for the diagonal stripe state (a) and the vertical stripe state (b) under a fixed electron filling ($n=0.875$ and a system size 16×16 sites).

mean field Hamiltonian (2) restores the electron- hole symmetry, thus yielding the symmetric band about its center if we disregard the CDW order parameter, $\langle\rho_i\rangle=0$. We also display the band structure for the vertical stripe state for comparison; The midgap band is substantially wider while the main SDW gap remains same as in the diagonal state.

The filling dependence of the band structure under a fixed $u(=8.0)$ is shown in Fig. 7. The main gap structure is hardly changed as the number of holes increases. As doping proceeds, excess carriers are accommodated into the midgap band. Note that this feature is very

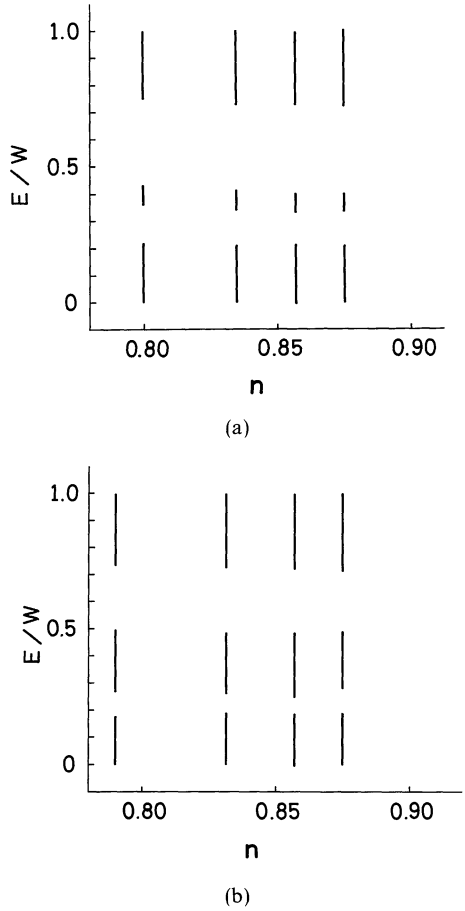

Fig. 7. The electron filling dependence of the band structures under a fixed value of $u(=8.0)$ near the half-filling. (a) The diagonal stripe state. (b) The vertical stripe state. The total band width is W.

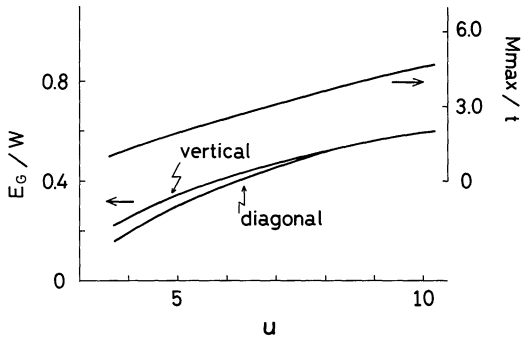

Fig. 8. The u-dependences of the main gap value E_G normalized by W for the diagonal and vertical states and the u-dependence of the maximum magnetization M_{max} normalized by the transfer integral t. The electron filling $n=0.875$ and system size 16×16 sites. Note that the E_G values for $n=0.875$ are the same for $n=0.857$ in this scale.

reminiscent of the optical absorption measurement by Suzuki[17] on (La, Sr)CuO_4 where under Sr doping the absorption intensity of the midgap band increases while the main gap structure remains unchanged. This characteristic band structure is effective in order to maximally save the loss of the SDW condensation energy upon doping. The present midgap structure resembles to that in the incommensurate CDW[18] and SDW states[4] of one dimensional systems.

We plot the U-dependence of the main SDW gap E_G defined by the energy difference between the top of the valence band and the bottom of the conduction band under a fixed filling ($n=0.875$ and 0.857) in Fig. 8. In the weak coupling region the vertical stripe state has a larger main gap than that of the diagonal one. Above $u\sim8$ the gaps in both states acquire the same magnitude. This value $u\cong8.0$ does not neccessarily coincide with the critical value ($u\sim4.0$) of the stability crossover from the vertical to diagonal states mentioned before. In Fig. 8 we also plot the maximum amplitudes of the SDW modulation $\langle M_i\rangle$ in the diagonal and vertical stripe states, which coincide in this scale, as a function of U. These two quantities are roughly proportional to each other, suggesting that as in the simple antiferromagnetic state the amplitude of the magnitization directly corresponds to the main SDW gap.

In order to understand the energy gap structures of these states in reciprocal space, we performed additional calculations: Since we know the potential energy $U\langle n_{i-\sigma}\rangle$ felt by a spin-σ electron at a site i in direct space, we obtain the Fourier components Δ_k as defined by

$$\Delta_{k\sigma}=U\sum_i\langle n_{i-\sigma}\rangle\, e^{ikR_i}, \tag{7}$$

where $k=lQ$ $(l=1, 2, \cdots, N)$. As we can choose $\Delta_{lQ\sigma}$ as real, the mean field Hamiltonian in reciprocal space is written as

$$H=\sum_{k\sigma}\varepsilon(k)c^{\dagger}_{k\sigma}c_{k\sigma}+\sum_{l=1}^{N/2}\sum_{k\sigma}\Delta_{lQ\sigma}\{c^{\dagger}_{k+lQ\sigma}c_{k\sigma}+\text{h.c.}\}. \tag{8}$$

By using only these Fourier components which

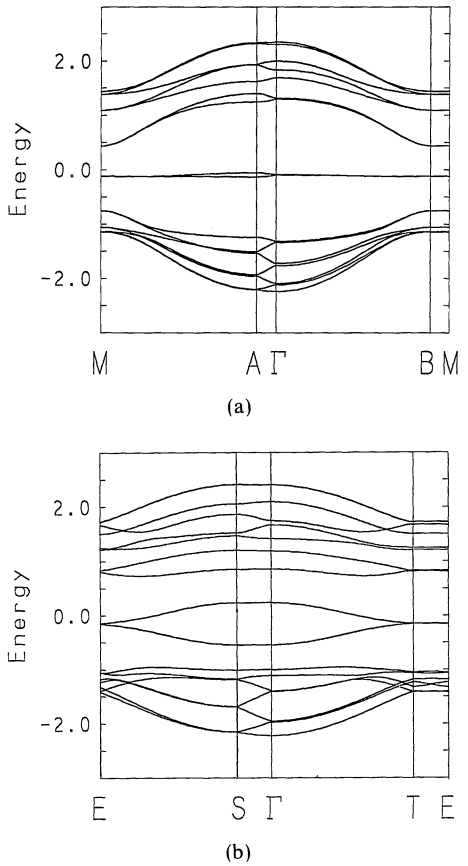

Fig. 9. The dispersion curves along the symmetry lines in the reduced zone scheme where the energy is normalized by t. $u=4.0$ and the filling $n=0.875$ with the system size $N\times N$ sites ($N=16$). The diagonal stripe state. Γ; $(k_x, k_y)=(0, 0)$ A; $((1/N), (1/N))$, B; $((\pi/2), -(\pi/2))$ and M; $((\pi/2)+(\pi/N), -(\pi/2)+(\pi/N))$. (b) The vertical stripe state. T; $((\pi/2)+(2\pi/N^2), 0)$ E; $((\pi/2)-(2\pi/N^2), (2\pi/N))$ and S; $(0, (2\pi/N))$.

is equivalent to assuming a complete periodic pattern of the spatial modulation, we again diagonalize the Hamiltonian matrix and obtain the dispersion relations, which yield the energy gap structure in reciprocal space. We illustrate some examples of the calculated results in Fig. 9 where the dispersion relations are plotted along the symmetry lines in the reduced zone scheme: In both cases diagonal (a) and vertical (b), the occupied valence band are separated by a wide gap, leaving no Fermi surface because the Fermi level lies in the gap and making these states an insulator. This midgap band in the diagonal state (a) is narrower than the in the vertical state (b), coinciding with the earlier result of the direct space diagonalization.

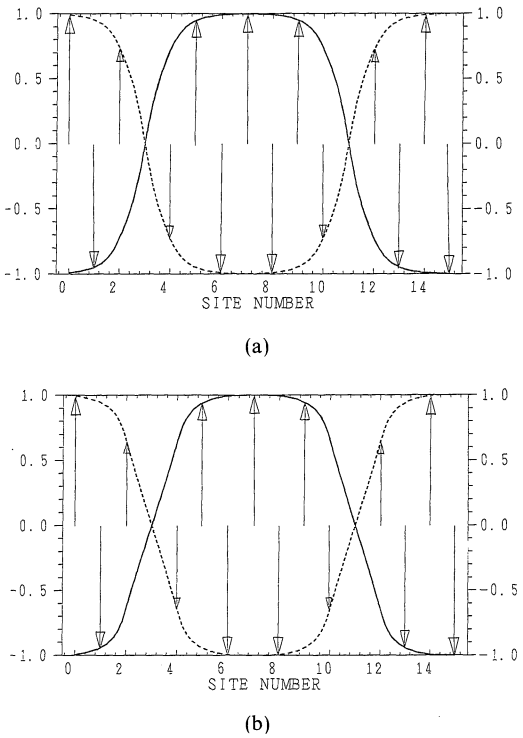

Fig. 10. The spatial profiles of the magnetization normalized by its maximum value as a function of lattice sites plotted along y axis. $u=6.0$, $n=0.875$ and the system size 16×16 sites. (a) The diagonal stripe state. (b) The vertical stripe state.

5.2 *Spatial pattern*

In Fig. 10 we plot the spatial profiles of the spin modulations as a function of lattice sites plotted along y axis for (a) the diagonal and (b) vertical stripe states: The envelope function of the magnetization is not simple sinusoidal but a more distorted wave form. Since our system sizes treated are limited, it is hard to determine precisely its functional form. We suggest that the wave form is reminiscent of the Jaccobi elliptic function $sn(x, k)$, which was the form in one dimensional CDW or SDW systems near the half-filling.[4,17] The wave length λ of the diagonal state is linearly related to the hole number: $\lambda_{\mathrm{SDW}}^{-1}\propto 1-n$.

In Fig. 11 we show the charge density pro-

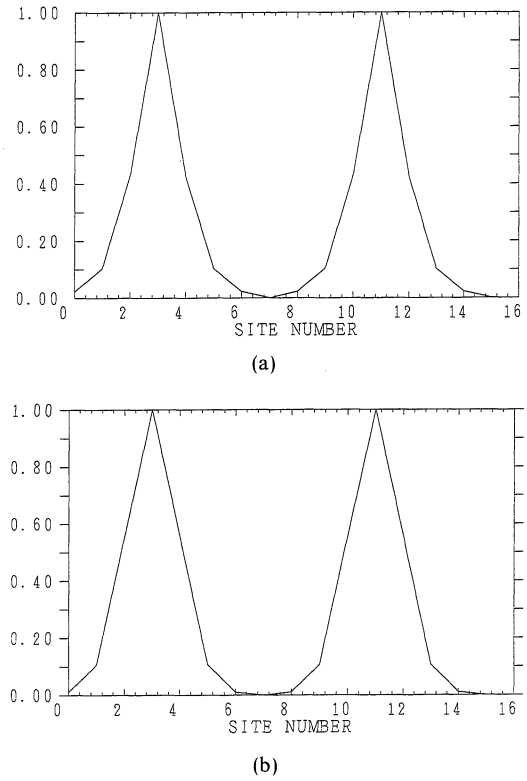

Fig. 11. The spatial profiles of the charge density $\delta\rho_i$ normalized by its maximum value as a function of lattice sites plotted along y axis. The parameter values used are same as in Fig. 10. (a) The diagonal stripe state. (b) The vertical stripe state.

files as a function of lattice sites plotted along y axis for (a) the diagonal and (b) the vertical stripe states where the set of the parameters used is the same as in Fig. 10. The accompanied CDW is found to be simply given by $\lambda_{\mathrm{CDW}}=\lambda_{\mathrm{SDW}}/2$. We suggest that the CDW modulation shown in Fig. 11 is roughly related to $sn^2(x, k)$, which was the case in one dimensional SDW and CDW near the half filling.[4,18]

§6. Conclusion

We have investigated the Hubbard model in two dimensions with a nearly half-filled band within the mean field approximation. By diagonalizing numerically the mean field Hamiltonian for finite system sizes we obtained several more stable magnetic states which are spatially modulated than the simple uniform antiferromagnetic state, when the fillings are away from the exactly half-full. We summarize our main results:

(1) The stable stripe states either diagonal or vertical consist of periodically placed domain walls between which almost antiferromagnetic state is realized, in other words these states are the soliton lattice state propagated perpendicularly to the modulation vector.

(2) Excess carriers are accommodated in the domain walls and localized in space, forming the midgap band. Therefore the gap structure consists of the main SDW gap inside which the midgap band is situated. The Fermi level lies inside the gap. The system is insulating. Main effect of doping (or changing carrier number of the system) is to increase the density of states of the midgap band.

(3) There is no stable region for the simple antiferromagnetic state where we have checked. In the weak coupling region around $U/t\lesssim 4$ the vertical stripe state is most stable while the diagonal stripe state is stabilized in the intermediate coupling region as shown in Fig. 5. The stability of the double Q cross stripe state is always intermediate between them.

(4) The wave length λ_{SDW} of the single Q states is proportional to the deviation from the half-filling; $|1-n|$. The accompanied charge density modulation is characterized by $\lambda_{\mathrm{SDW}}/2$.

Finally let us briefly discuss some relevance to the high T_c oxide systems:

(1) The observed quasi-static incommensurate magnetic fluctuations[1] in (La, Sr)CuO_4 are reminiscent of the present modulated magnetic state.

(2) The gradual change of the magnetic moment upon doping in (La, Sr)CuO_4 observed by μSR[19] and the nuclear specific heat experiment[20] is in accord with the present itinerant electron picture.

(3) The optical measurement[17] detects the large midgap absorption inside the main energy gap in (La, Sr)CuO_4 which can be interpreted as the midgap band.

Since the actual oxide system might belong to more strongly correlated regime where the present approximation is not fully reliable, it is to be seen what aspects remain when taking into account correlation effects.

Acknowledgments

The authors thank M. Nakano for useful discussions. One of the authors (H.N.) is supported in part by the National Science Foundation under Grant No. PHY82-17853, supplemented by funds from the National Aeronautics and Space Administration.

References

1) G. Shirane, R. J. Birgeneau, Y. Endoh, P. Gehring, M. A. Kastner, K. Kitazawa, H. Kojima, I. Tanaka, T. R. Thurston and K. Yamada: Phys. Rev. Lett. **63** (1989) 330; Also see H. Yoshizawa, S. Mitsuda, H. Kitazawa and K. Katsumata: J. Phys. Soc. Jpn. **57** (1988) 3686.
2) D. R. Penn: Phys. Rev. **142** (1966) 350.
3) See for example, E. Fawcett: Rev. Mod. Phys. **60** (1988) 209.
4) K. Machida and M. Fujita: Phys. Rev. B**30** (1984) 5284; Also see, K. Machida: Physica C**158** (1989) 192.
5) W. P. Su: Phys. Rev. B**37** (1988) 9904; W. P. Su and X. Y. Chen: Phys. Rev. B **38** (1988) 8879, H.-Y. Choi and E. J. Mele: Phys. Rev. B**38** (1988) 4540.
6) J. R. Schrieffer, X.-G. Wen and S.-C. Zhang: Phys. Rev. Lett. **60** (1988) 944.
7) D. Poilblanc and T. M. Rice: Phys. Rev. B**39** (1989) 9749.
8) H. J. Schulz: J. Phys. France **50** (1989) 2833.
9) J. Zaanen and O. Gunnarsson: Phys Rev. B**40** (1989) 7391.
10) M. Imada and Y. Hatsugai: J. Phys. Soc. Jpn. **58** (1989) 3752.
11) J. E. Hirsch and S. Tang: Phys. Rev. Lett. **62** (1989) 591.
12) J. E. Hirsch: Phys. Rev. B**31** (1985) 4403.
13) S. R. White, D. J. Scalapino, R. L. Sugar, E. Y. Loh, J. E. Gubernatis and R. T. Scalettar: Phys. Rev. B**40** (1989) 506.
14) E. W. Fenton: J. Phys. F **6** (1976) 2403.
15) D. W. Buker: Phys. Rev. B**25** (1982) 991.
16) Also see for non-collinear multiple Q states; A. Yoshimori and S. Inagaki: J. Phys. Soc. Jpn. **44** (1978) 101; T. Jo and K. Hirai: J. Phys. Soc. Jpn. **53** (1984) 3183; M. W. Long: J. Phys. C**1** (1989) 2857; C. L. Henley: Phys. Rev. Lett. **62** (1989) 2056.
17) M. Suzuki: Phys. Rev. B**39** (1989) 2312.
18) M. Nakano and K. Machida: Phys. Rev. B**33** (1986) 6718; K. Machida and M. Nakano: Phys. Rev. B**34** (1986) 5073.
19) A. Weidinger, Ch. Niedermayer, A. Golnik, R. Simon, E. Recknagel, J. I. Budnick, B. Chamberland and C. Baines: Phys. Rev. Lett. **62** (1989) 102.
20) N. Wada, H. Muro-oka, Y. Nakamura and K. Kumagai: Physica C**157** (1989) 453.